

## IRREGULAR MASS TRANSFER IN THE POLARS VV PUPPIS AND V393 PAVONIS DURING THE LOW STATE

DIRK PANDEL

Department of Physics, University of California, Santa Barbara, CA 93106; dpandel@xmmom.physics.ucsb.edu

AND

FRANCE A. CÓRDOVA

Institute of Geophysics and Planetary Physics, Department of Physics, University of California, Riverside, CA 92521

Received 2004 September 16; accepted 2004 October 25

### ABSTRACT

The polars VV Pup and V393 Pav were observed with *XMM-Newton* during states of low accretion with peak X-ray luminosities of  $\sim 1 \times 10^{30}$  and  $\sim 1 \times 10^{31}$  ergs s<sup>-1</sup>, respectively. In both polars, accretion onto the white dwarf was extremely irregular, and the accretion rate varied by more than 1 order of magnitude on timescales of  $\sim 1$  hr. Our observations suggest that this type of irregular accretion is a common phenomenon in polars during the low state. The likely cause of the accretion rate fluctuations is coronal mass ejections or solar flares on the companion star that intermittently increase the mass transfer into the accretion stream. Our findings demonstrate that the companion stars in cataclysmic variables possess highly active atmospheres.

*Subject headings:* accretion, accretion disks — binaries: close — novae, cataclysmic variables — stars: individual (VV Puppis, V393 Pavonis) — stars: magnetic fields — X-rays: binaries

### 1. INTRODUCTION

AM Her binaries or polars are cataclysmic variables in which the strong magnetic field of the white dwarf primary prevents the formation of an accretion disk (e.g., Warner 1995). The accretion stream from the Roche lobe–filling companion star follows the magnetic field lines and impacts the white dwarf near a magnetic pole. There the accreting gas forms a standoff shock and is heated to temperatures in excess of  $10^8$  K. As the shock-heated gas in the accretion column settles onto the white dwarf, it cools via the emission of cyclotron radiation (infrared to ultraviolet) and bremsstrahlung (X-rays). In the absence of an accretion disk, matter is transported directly from the companion star to the white dwarf, and the observed X-ray luminosity is a direct measure of the rate at which the companion star transfers mass into the accretion stream.

Many polars have been observed to enter low states during which little or no emission from the accretion column is seen and which can last from several days to years. While the cause of these low states is not known, they must be connected to a reduction of the mass transfer rate from the companion star. In the past, studying the weak X-ray emission from low-state polars has been difficult, but the high sensitivity of the new generation of X-ray telescopes promises new insights into the underlying physics. A first *XMM-Newton* observation of a polar during the low state revealed strong flaring at X-ray and ultraviolet (UV) energies in UZ For (Pandel & Córdoba 2002). In this paper, we present *XMM-Newton* data for the two polars VV Pup and V393 Pav, which were observed during their low states.

VV Pup is the third cataclysmic variable that was identified as an AM Her–type binary (Tapia 1977). It has been extensively studied at infrared, optical, UV, and X-ray wavelengths. VV Pup has a short orbital period of 100.43546 minutes (Schneider & Young 1980). It is optically faint, with *V* magnitudes in the range 14.5–18 (Downes et al. 2001) and is located at a distance of  $\sim 144$  pc (Bailey 1981). The primary and secondary poles have magnetic field strengths of 31 and 54 MG, respectively (Schwope & Beuermann 1997). V393 Pav (RX J1957.1–5738), which was

discovered in the *ROSAT* All Sky Survey, has an orbital period of 98.8194 minutes, a distance of  $\sim 350$  pc, and a magnetic field strength of 16 MG at the primary pole (Thomas et al. 1996). In both polars, the main accretion region is obscured by the white dwarf during roughly half of the orbital cycle, thus causing the X-ray flux to be strongly modulated at the orbital period.

### 2. OBSERVATIONS AND DATA REDUCTION

VV Pup was observed with *XMM-Newton* (Jansen et al. 2001) on 2002 November 11. We obtained 18.0 ks of continuous X-ray data from the two EPIC MOS cameras (Turner et al. 2001) and 20.4 ks from the EPIC pn camera (Strüder et al. 2001). The three instruments were operated with the thick blocking filters and the CCDs in small window mode. The Optical Monitor (Mason et al. 2001) performed six exposures with a total duration of 23.2 ks using the UVW1 filter (240–340 nm). The Optical Monitor was operated in fast mode with a sample time of 0.5 s.

V393 Pav was observed on 2003 October 19. We obtained 23.4 ks of X-ray data from the EPIC MOS cameras and 23.2 ks from the EPIC pn camera. The two EPIC MOS cameras were operated in large window mode and the EPIC pn camera in small window mode. Thin blocking filters were used for all three instruments. The Optical Monitor performed five exposures in fast mode with a total duration of 18.2 ks using the UVW1 filter. Because of the low signal-to-noise ratio, we did not use the data from the Reflection Grating Spectrometer (RGS; den Herder et al. 2001) for either of the two observations.

We extracted source photons from the EPIC MOS and pn data using a circular aperture with a radius of  $15''$ . The count rates given in this paper have been corrected for the 65% enclosed energy fraction of this aperture. We included in our analysis good photon events (FLAG = 0) in the energy range 0.2–12 keV with patterns 0–12 for EPIC MOS and 0–4 for EPIC pn. To create X-ray light curves, we applied a barycentric correction to the photon arrival times and summed the count rates from all three EPIC instruments. Background rates were estimated from larger

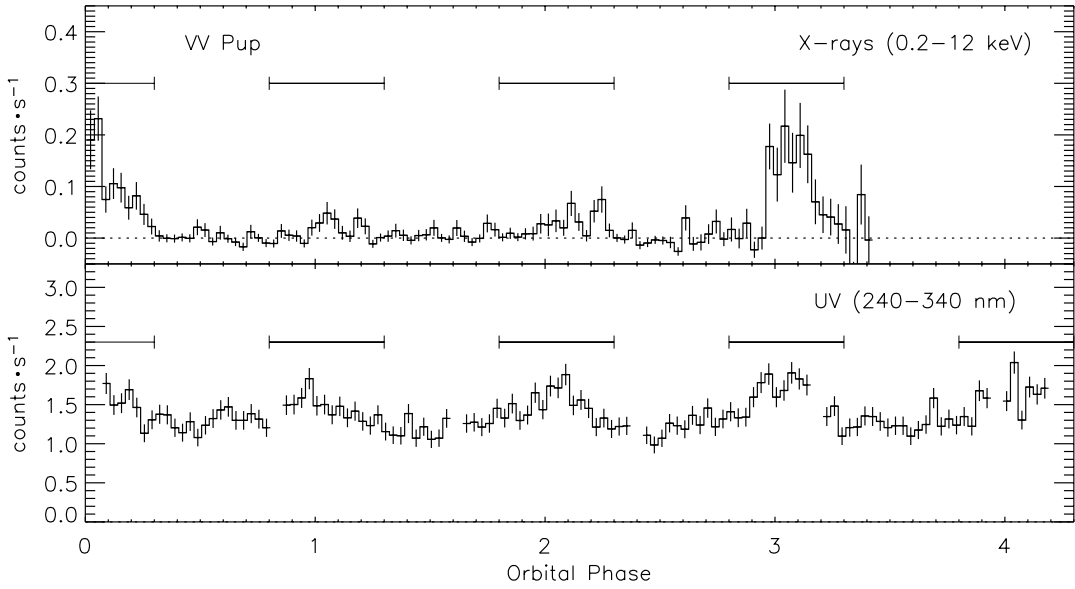


FIG. 1.—X-ray and UV light curves of VV Pup (orbital period 100.43546 minutes). Orbital phase zero is defined as BJD(TT) 2452619.780, the time of maximum optical light as predicted by the ephemeris in Walker (1965). The horizontal bars indicate the time periods during which the main accretion region is visible.

regions on the same CCD as the source image. During the VV Pup observation, background contributed  $\sim 0.01 \text{ s}^{-1}$  to the count rate in the source aperture, except during the last 5000 s, when the background rate increased considerably and reached up to  $0.15 \text{ s}^{-1}$ . During the V393 Pav observation, the background rate was fluctuating between 0.01 and  $0.05 \text{ s}^{-1}$ . We extracted source photons from the Optical Monitor data using a circular aperture of  $5''$  radius, which encloses 81% of the source photons in the UVW1 filter. The UV background rate was  $\sim 0.5 \text{ s}^{-1}$  during both observations, which amounts to  $\sim 25\%$  for VV Pup and  $\sim 70\%$  for V393 Pav.

### 3. X-RAY AND UV LIGHT CURVES

X-ray and UV light curves obtained from the *XMM-Newton* data are shown in Figures 1 and 2. The X-ray light curves show

the sum of the count rates in the three EPIC cameras. In the UV light curves, a count rate of  $1 \text{ s}^{-1}$  corresponds to a flux of  $0.13 \text{ mJy}$  at  $290 \text{ nm}$ . For VV Pup, we defined as orbital phase zero BJD(TT) 2452619.780 (Barycentric Julian Date in Terrestrial Time), which is the time of maximum optical light as predicted by the ephemeris in Walker (1965). This ephemeris has an accumulated uncertainty of 0.1 in phase. For V393 Pav, we defined as orbital phase zero BJD(TT) 2452931.932, the time of inferior conjunction of the secondary as predicted by the ephemeris in Thomas et al. (1996). The accumulated uncertainty of this ephemeris is 0.15 in phase.

*XMM-Newton* observed the two polars during states of low accretion with X-ray luminosities considerably lower than previously seen. *ROSAT* observations of VV Pup (Ramsay et al. 1996) found the polar in a very bright state with an X-ray

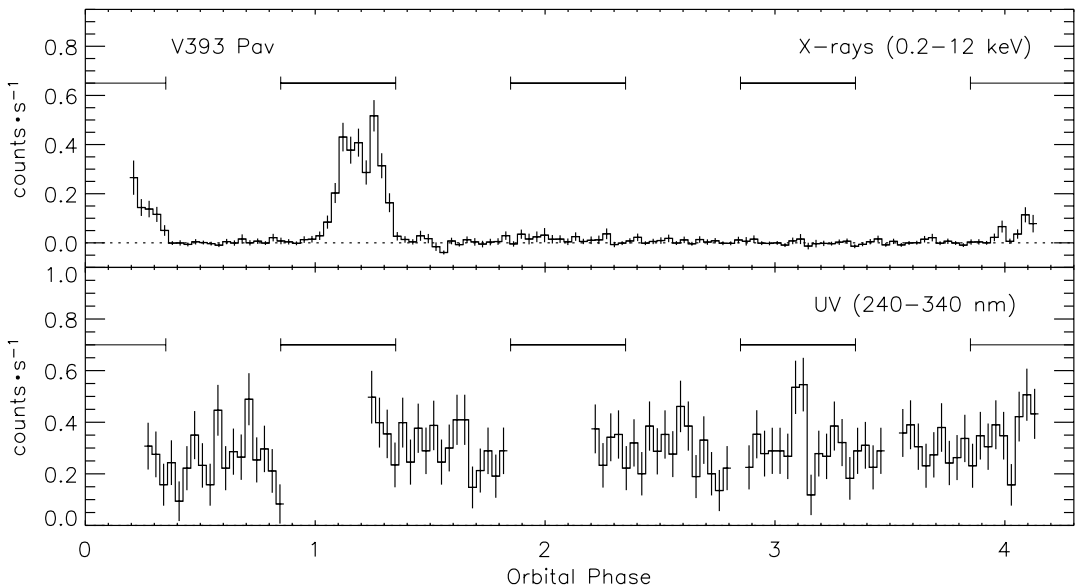


FIG. 2.—X-ray and UV light curves of V393 Pav (orbital period 98.8194 minutes). Orbital phase zero is defined as BJD(TT) 2452931.932, the time of inferior conjunction of the secondary as predicted by the ephemeris in Thomas et al. (1996). The horizontal bars indicate the time periods during which the main accretion region is visible.

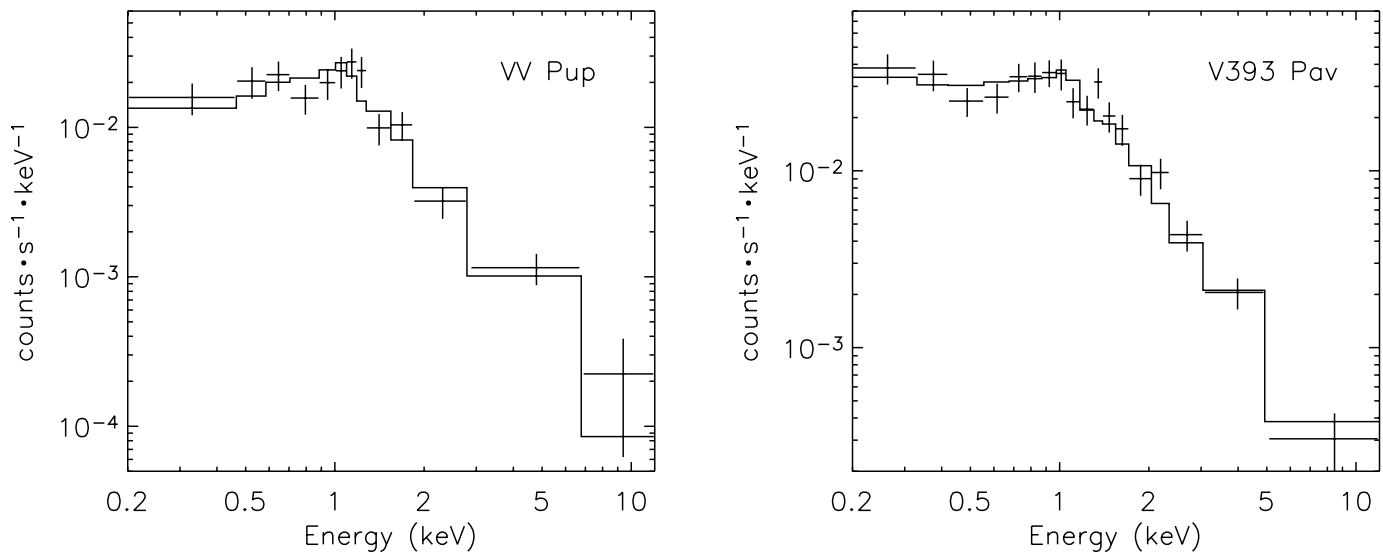


Fig. 3.—Average X-ray spectra during the bright phases. Shown are the combined spectra of the three EPIC detectors averaged over the bright phase time intervals indicated by the horizontal bars in Figs. 1 and 2. The solid lines show the best fit with a cooling flow model.

flux that would have produced a peak count rate of  $40 \text{ s}^{-1}$  in *XMM-Newton*. This is  $\sim 200$  times higher than the peak count rate we observed. The X-ray flux detected with *ROSAT* from V393 Pav (Thomas et al. 1996) corresponds to an *XMM-Newton* peak count rate of  $3 \text{ s}^{-1}$ , which is a factor of 8 higher than that during our observation.

For our choice of orbital phase zero, the bright phases, i.e., the time periods during which the main accretion region is visible, are expected to last from phase  $-0.3$  to  $0.2$  in both polars (Patterson et al. 1984; Thomas et al. 1996). Figures 1 and 2 show that the X-ray emission is mostly limited to this phase range. Note that the actual bright phases appear to end slightly later than the predicted phase  $0.2$ . This delay is, however, within the uncertainty of the ephemerides. We therefore assumed that the bright phases in VV Pup and V393 Pav occur later than predicted by  $0.1$  and  $0.15$ , respectively. The bright phases are then expected to last from  $-0.2$  to  $0.3$  and  $-0.15$  to  $0.35$ , respectively (indicated by horizontal bars in Figs. 1 and 2).

For VV Pup, the more recent UV light curve in Vennes et al. (1995) shows that, consistent with earlier observations, the bright phase ends at  $\sim 0.2$ . This indicates that no significant phase change relative to the ephemeris in Walker (1965) has occurred. Therefore, the delay of the bright phase by  $\sim 0.1$  during our observations is probably not due to the uncertainty of the ephemeris. The delay may, however, be the result of an accretion-rate-dependent change in the longitude of the accretion region. Such a longitude change has been observed in the polar WW Hor by Pandel et al. (2002), who found that, during an intermediate accretion state, the bright phase was delayed by  $0.04$  compared to the high state. Similar to WW Hor, the delay of the bright phase in VV Pup may have been caused by the very low accretion rate during our observation.

X-ray emission from both polars is only seen during the bright phases, which indicates that the main accretion region is the source of the X-rays. We find that the X-ray flux integrated over the faint phases, i.e., the time periods during which the accretion region is not visible ( $0.3$ – $0.8$  for VV Pup and  $0.4$ – $0.8$  for V393 Pav), is consistent with zero emission. This implies an upper limit of  $0.003 \text{ s}^{-1}$  on the average count rate during the faint phases (at 90% confidence level). The X-ray flux observed

during the bright phases is not constant but varies greatly by 1 order of magnitude or more on timescales of  $\sim 1$  hr. The probable cause of these brightness fluctuations is a highly variable accretion rate.

The UV light curves in Figures 1 and 2 show considerably less variability than the X-ray light curves. In particular, the large increases of the X-ray flux do not appear to be accompanied by enhanced UV emission. The observed UV flux is most likely thermal radiation from the white dwarf. On average, *XMM-Newton* detected UV fluxes of  $1.4 \text{ s}^{-1}$  ( $0.18 \text{ mJy}$ ) for VV Pup and  $0.30 \text{ s}^{-1}$  ( $0.039 \text{ mJy}$ ) for V393 Pav. For an assumed white dwarf radius of  $8 \times 10^8 \text{ cm}$ , the UV fluxes are consistent with blackbody radiation from white dwarfs with temperatures of  $11,000$  and  $11,500 \text{ K}$ , respectively. These temperatures are similar to those typically found for polars (e.g., Sion 1999). The UV light curve of VV Pup shows a 30% orbital modulation that peaks around phase  $0.0$ , near the center of the bright phase. The modulation is likely due to a higher temperature of the white dwarf around the main accretion region. No orbital modulation is seen for V393 Pav.

#### 4. X-RAY SPECTRA

Figure 3 shows the X-ray spectra of VV Pup and V393 Pav averaged over the bright phase time intervals (indicated by the horizontal bars in Figures 1 and 2). X-ray emission from polars during the high-luminosity state typically consists of a strong blackbody component at low energies and a weak bremsstrahlung component that is visible only at high energies. In V393 Pav, the blackbody component dominated the spectrum below  $0.6 \text{ keV}$  during a previous X-ray observation (Thomas et al. 1996). The bremsstrahlung is thought to be emission from the shock-heated plasma in the accretion column, while the blackbody radiation is due to reprocessing of hard X-rays in the white dwarf's atmosphere around the accretion region. In contrast to the high state, the spectra in Figure 3 show no evidence of a soft blackbody component. It is likely that, owing to the low accretion rates, the blackbody temperature was reduced, and the blackbody distribution was shifted out of the detector bandpass. The X-ray emission detected by *XMM-Newton* appears to be solely due to the optically thin, cooling plasma in the accretion column.

TABLE 1  
SPECTRAL FIT PARAMETERS

Object	Model	$kT$ (keV)	EM ( $10^{52}$ cm $^{-3}$ )	$\dot{M}$ ( $10^{13}$ g s $^{-1}$ )	$L_{\text{bol}}$ ( $10^{30}$ ergs s $^{-1}$ )	$C$ -statistic (858 bins)
VV Pup .....	Bremsstrahlung	$2.7^{+1.4}_{-0.8}$	$9.7 \pm 1.5$	...	1.23	619
	MEKAL	$3.4^{+1.0}_{-0.8}$	$6.5 \pm 0.8$	...	1.32	610
	Cooling flow	$9.9^{+6.8}_{-3.4}$	...	$3.8 \pm 1.2$	1.46	612
V393 Pav .....	Bremsstrahlung	$4.5^{+1.8}_{-1.1}$	$81 \pm 7$	...	13.1	639
	MEKAL	$4.5^{+1.4}_{-1.0}$	$61 \pm 5$	...	13.8	639
	Cooling flow	$17.1^{+11.4}_{-5.8}$	...	$25 \pm 7$	16.6	637

NOTES.—The table shows the best-fit parameters for three spectral models (see § 4). The parameters shown are the plasma temperature  $kT$ , the emission measure EM, the accretion rate  $\dot{M}$ , the bolometric luminosity  $L_{\text{bol}}$ , and the likelihood according to the  $C$ -statistic (for assumed distances, see § 1). Note that for the cooling flow model  $kT$  is the maximum or initial temperature of the flow. The values of EM,  $\dot{M}$ , and  $L_{\text{bol}}$  have been normalized to count rates of  $0.2$  s $^{-1}$  for VV Pup and  $0.4$  s $^{-1}$  for V393 Pav.

Spectral fitting was performed with the XSPEC package, version 11.2 (Arnaud 1996). We binned the spectra at one-third of the FWHM detector resolution and performed simultaneous fits to the data from all three EPIC cameras. To account for the low number of counts per bin, we used the  $C$ -statistic (Cash 1979). We fitted the spectra with three different models: a single-temperature bremsstrahlung model, the MEKAL model for an optically thin and collisionally ionized plasma based on calculations by Mewe et al. (1985) and Liedahl et al. (1995), and a simple cooling flow model according to Mushotzky & Szymkowiak (1988). Whereas the first two models assume a single plasma temperature  $T$ , the latter model describes an isobaric cooling flow with a continuous temperature distribution. We calculated the model spectrum of the cooling flow by adding single-temperature MEKAL models on a grid with spacing 0.1 in  $\log T$ . Each of the three models has two free parameters. They are, for the bremsstrahlung and MEKAL models, the temperature  $kT$  and the emission measure EM and, for the cooling flow model, the maximum or initial temperature  $kT$  and the mass accretion rate  $\dot{M}$ . To calculate emission measures, accretion rates, and luminosities, we assumed isotropic emission and neglected reflection of X-rays by the white dwarf. As distances to the polars, we used those given in § 1. For the MEKAL and the cooling flow models, we fixed elemental abundances at the solar values in Anders & Grevesse (1989).

The best-fit parameters for the three models are shown in Table 1. The likelihood values of the  $C$ -statistic are very close and do not favor a particular model, although the multi-temperature cooling flow is probably the most appropriate model for the accretion column. The  $C$ -statistic does not provide a measure for the quality of the fit. However, if the spectra are rebinned, as shown in Figure 3, the  $\chi^2$ -statistic can be used, and we find good agreement between the data and the cooling flow model with  $\chi^2(\text{dof}) = 12.8(11)$  for VV Pup and  $16.3(16)$  for V393 Pav. Our estimates for the bolometric luminosity  $L_{\text{bol}}$  are fairly model independent, since most of the X-ray flux is inside the 0.2–12 keV range and directly detected by *XMM-Newton*. Note that EM,  $\dot{M}$ , and  $L_{\text{bol}}$  have been normalized to count rates of  $0.2$  s $^{-1}$  (VV Pup) and  $0.4$  s $^{-1}$  (V393 Pav), which correspond approximately to the peaks of the light curves in Figures 1 and 2. Adding interstellar absorption to the spectral model did not improve the quality of the fit. This establishes upper limits of  $1 \times 10^{20}$  cm $^{-2}$  for VV Pup and  $2 \times 10^{20}$  cm $^{-2}$  for V393 Pav on the neutral hydrogen column density  $N_{\text{H}}$ . For VV Pup, this is consistent with a previously found upper limit of  $1 \times 10^{19}$  cm $^{-2}$  (Ramsay et al. 1996).

## 5. DISCUSSION

Both polars were observed with *XMM-Newton* during states of low accretion. With a peak X-ray luminosity of  $\sim 1 \times 10^{30}$  ergs s $^{-1}$ , VV Pup was more than 2 orders of magnitude fainter than during a previous high-state observation (Ramsay et al. 1996). For V393 Pav, we derived a peak X-ray luminosity of  $\sim 1 \times 10^{31}$  ergs s $^{-1}$ . Compared to the only previous X-ray observation (Thomas et al. 1996), the polar was about 1 order of magnitude fainter. The *XMM-Newton* spectra show no evidence of the soft blackbody component due to X-ray reprocessing that is typically seen in polars during the high state. Owing to the low accretion rates, this blackbody radiation was probably emitted at a lower temperature, outside the *XMM-Newton* bandpass.

In both polars, X-ray emission was only seen during the bright phases, while no emission was detected during the faint phases. This clearly shows that the X-rays originated from the main accretion region on the white dwarf. Furthermore, the X-ray spectrum is consistent with emission from the shock-heated, optically thin plasma in the accretion column. As shown in Figures 1 and 2, the X-ray luminosity of the accretion region was fluctuating by more than 1 order of magnitude on timescales of  $\sim 1$  hr. In the absence of an accretion disk, these luminosity changes must be due to a strongly varying mass transfer rate from the companion star into the accretion stream.

Large brightness fluctuations during the low state, other than the orbital modulations, have been observed in a few polars. However, in only one case could these variations be unambiguously attributed to irregular mass transfer from the companion star. Pandel & Córdova (2002) observed a flare with *XMM-Newton* during an extremely low accretion state of UZ For. The flare, which lasted  $\sim 1000$  s, increased the X-ray flux by a factor of  $\sim 30$  and was also detected in the UV. The authors showed that the flare was caused by an accretion event on the white dwarf following an intermittent increase in the mass transfer rate from the companion star. Similar transient events have been observed by Warren et al. (1993) with the *Extreme Ultraviolet Explorer* in the polar QS Tel. As possible causes, the authors suggested a varying mass transfer rate, filaments in the accretion stream, and solar flares on the companion star. Bonnet-Bidaud et al. (2000) observed small optical flares (0.3–0.5 mag) in AM Her during a low state. These flares were probably caused by either accretion rate fluctuations or instabilities in the accretion stream. Also for AM Her, Shakhovskoy et al. (1993) reported a large optical transient ( $\sim 2$  mag). The properties of the transient (exponential decay, blue color, no polarization)

suggest emission from a solar flare on the companion star. A solar flare was probably also responsible for an optical transient ( $\sim 1$  mag in  $B$ ) observed in the low accretion rate polar HS 1023+3900 by Schwarz et al. (2001).

Polars are known to exhibit strong flaring during high accretion states (e.g., Cropper & Warner 1986). These brightness fluctuations are probably caused by dense blobs or filaments in the accretion stream (Kuijpers & Pringle 1982; Frank et al. 1988). Some of the flaring observed during high states may be due to irregular mass transfer from the companion star. However, it is difficult to distinguish these brightness variations from those caused by inhomogeneities in the accretion stream. Moreover, if the accretion rate fluctuations are of similar magnitude to those during the low state, they will be small compared to the average high-state accretion rate and probably undetectable.

The *XMM-Newton* observations of the three polars VV Pup, V393 Pav, and UZ For demonstrate that extremely irregular mass transfer is a common phenomenon in polars during the low state. While the causes of low states in polars are poorly understood, it is clear that they must be due to variations of the rate at which the companion star transfers mass into the accretion stream near the L1 Lagrange point. Variations in the size of the Roche lobe occur on timescales of  $10^4$ – $10^5$  yr (King et al. 1995; Ritter 1988) and cannot be responsible for the low states. It has been suggested that starspots can pass under the L1 point and greatly reduce the mass transfer rate (Livio & Pringle 1994; King & Cannizzo 1998; Hessman et al. 2000). However, Howell et al. (2000) showed that, in short-period cataclysmic variables, the critical Roche surface is well above the photosphere, so that the mass flow through the L1 point is actually controlled by the magnetic activity in the chromosphere. In both scenarios, coronal mass ejections or solar flares near the L1 point can lead to an intermittent increase of the mass transfer rate on short timescales, thus causing the X-ray flaring observed in the three polars. The irregular mass transfer seen during low states provides evidence of a highly active stellar atmosphere near the L1 point.

Little is known about the level of stellar activity on the companion stars of cataclysmic variables, yet their rapid rotation, which is synchronized with the binary orbital motion, suggests that they are highly active. Evidence of starspots and magnetic flares on the companion stars has been found in a few cataclysmic variables (e.g., Howell et al. 2000; Webb et al. 2002; Shakhovskoy et al. 1993). From our accretion rate measurements (Table 1), we estimate that the large X-ray flares shown in Figures 1 and 2 were caused by accretion of  $\sim 5 \times 10^{16}$  g (VV Pup) and  $\sim 5 \times 10^{17}$  g (V393 Pav) of gas onto the white dwarf. These masses are consistent with those of solar flares on active M dwarfs, which are in the range  $10^{15}$ – $10^{18}$  g (derived from density and volume measurements in Pallavicini et al. 1990). Note, however, that the total accretion rates and therefore the flare masses may actually be higher than our estimates (see next paragraph). With the correction factors derived below, our flare mass estimates increase to  $\sim 10^{18}$  g, which is still within the mass range of solar flares on M dwarfs.

At the low accretion rates observed in the two polars, cooling in the accretion column is likely dominated by cyclotron radiation (e.g., Lamb & Masters 1979). Our measurements of  $L_{\text{bol}}$  and  $\dot{M}$ , which are solely based on the X-ray emission, may therefore be considerably below the total luminosities and accretion rates. A rough estimate of the total luminosity (X-ray plus cyclotron) can be obtained from the theoretical results in Woelk & Beuermann (1996). We estimate from their Figure 9 that the total  $L_{\text{bol}}$  and  $\dot{M}$  are higher than those in Table 1 by

a factor of  $\sim 20$  for VV Pup and  $\sim 3$  for V393 Pav. Here we assumed a typical fractional area of the accretion region  $f = 10^{-3}$  (e.g., Sirk & Howell 1998), a white dwarf mass of  $0.7 M_{\odot}$ , and a white dwarf radius of  $8 \times 10^8$  cm. The correction factors imply, for both polars, a specific accretion rate of  $\sim 0.1 \text{ g cm}^{-2} \text{ s}^{-1}$  at the peak of the light curves.

The X-ray flare observed in UZ For by Pandel & Córdoba (2002) was accompanied by a simultaneous UV flare probably due to cyclotron radiation. However, no such UV flaring is visible in the light curves of VV Pup and V393 Pav. Cyclotron radiation from polars is typically seen at optical and infrared wavelengths and only under certain conditions in the near UV. For a specific accretion rate  $\dot{m} \approx 0.1 \text{ g cm}^{-2} \text{ s}^{-1}$ , Figure 5 in Woelk & Beuermann (1996) indicates that the cyclotron flux at 290 nm ( $1.0 \times 10^{15}$  Hz) has already dropped well below the peak in the infrared, and it is probably much weaker than the thermal radiation from the white dwarf (not shown in the figure). We therefore do not expect to see significant cyclotron emission in the UV light curves of VV Pup and V393 Pav. In UZ For, some cyclotron radiation may have been emitted in the near UV because of the higher magnetic field strength ( $\sim 50$  MG) and possibly a smaller accretion region.

As indicated by the presence of a hot, X-ray-emitting plasma, the specific accretion rate  $\dot{m} \approx 0.1 \text{ g cm}^{-2} \text{ s}^{-1}$  places the two polars in the regime of a standoff shock (e.g., Woelk & Beuermann 1996). Recently, several polars have been discovered that appear to be in a permanent state of very low accretion with  $\dot{m} \approx 10^{-3} \text{ g cm}^{-2} \text{ s}^{-1}$  (Reimers et al. 1999; Reimers & Hagen 2000; Szkody et al. 2003). At this low  $\dot{m}$ , a standoff shock does not form, and accretion is instead characterized by the bombardment solution (Kuijpers & Pringle 1982; Rousseau et al. 1996). While these low accretion rate polars are strong emitters of cyclotron radiation, their X-ray emission is very weak. Unfortunately, the observational data on these objects are insufficient to determine whether they exhibit accretion rate fluctuations similar to those of VV Pup and V393 Pav. Variability studies of the low accretion rate polars could reveal a possible correlation between the average mass transfer rate and the level of stellar activity on the companion star.

## 6. CONCLUSIONS

*XMM-Newton* observations of VV Pup and V393 Pav found the polars in states of low accretion with peak X-ray luminosities of  $\sim 1 \times 10^{30}$  and  $\sim 1 \times 10^{31}$  ergs  $\text{s}^{-1}$ , respectively. In both polars, accretion onto the white dwarf was highly variable and fluctuated by more than 1 order of magnitude on timescales of  $\sim 1$  hr. All of the observed X-ray emission appears to originate from the main accretion region. The X-ray spectrum is consistent with emission from the shock-heated plasma in the accretion column but does not show evidence of the soft blackbody component that is commonly seen during high states. The UV flux is considerably less variable than the X-ray flux, and no brightness fluctuations simultaneous to those in the X-ray data are seen. For VV Pup, we found a 30% orbital UV modulation due to the heating of the polar region by the accretion stream.

From our observations of VV Pup and V393 Pav and from the *XMM-Newton* data of UZ For presented in Pandel & Córdoba (2002), it becomes evident that extremely irregular accretion is a common phenomenon in polars during the low state. In the absence of an accretion disk, the cause of these accretion rate fluctuations must be a strongly varying mass transfer rate from the companion star into the accretion stream. The large variations of the mass transfer rate are likely a result

of coronal mass ejections or solar flares near the L1 Lagrange point. Our findings demonstrate that the companion stars in cataclysmic variables possess highly active atmospheres. The high sensitivity of *XMM-Newton* provides a new way to study stellar activity on the companion stars in polars.

This work is based on observations obtained with *XMM-Newton*, an ESA science mission with instruments and contributions directly funded by ESA member states and the USA (NASA). The authors acknowledge support from NASA grant NAG5-12934.

## REFERENCES

- Anders, E., & Grevesse, N. 1989, *Geochim. Cosmochim. Acta*, 53, 197  
 Arnaud, K. A. 1996, in *ASP Conf. Ser. 101, Astronomical Data Analysis Software and Systems V*, ed. G. Jacoby & J. Barnes (San Francisco: ASP), 17  
 Bailey, J. 1981, *MNRAS*, 197, 31  
 Bonnet-Bidaud, J. M., et al. 2000, *A&A*, 354, 1003  
 Cash, W. 1979, *ApJ*, 228, 939  
 Cropper, M., & Warner, B. 1986, *MNRAS*, 220, 633  
 den Herder, J. W., et al. 2001, *A&A*, 365, L7  
 Downes, R. A., Webbink, R. F., Shara, M. M., Ritter, H., Kolb, U., & Duerbeck, H. W. 2001, *PASP*, 113, 764  
 Frank, J., King, A. R., & Lasota, J.-P. 1988, *A&A*, 193, 113  
 Hessman, F. V., Gänsicke, B. T., & Mattei, J. A. 2000, *A&A*, 361, 952  
 Howell, S. B., Ciardi, D. R., Dhillon, V. S., & Skidmore, W. 2000, *ApJ*, 530, 904  
 Jansen, F., et al. 2001, *A&A*, 365, L1  
 King, A. R., & Cannizzo, J. K. 1998, *ApJ*, 499, 348  
 King, A. R., Frank, J., Kolb, U., & Ritter, H. 1995, *ApJ*, 444, L37  
 Kuijpers, J., & Pringle, J. E. 1982, *A&A*, 114, L4  
 Lamb, D. Q., & Masters, A. R. 1979, *ApJ*, 234, L117  
 Liedahl, D. A., Osterheld, A. L., & Goldstein, W. H. 1995, *ApJ*, 438, L115  
 Livio, M., & Pringle, J. E. 1994, *ApJ*, 427, 956  
 Mason, K. O., et al. 2001, *A&A*, 365, L36  
 Mewe, R., Gronenschild, E. H. B. M., & van den Oord, G. H. J. 1985, *A&AS*, 62, 197  
 Mushotzky, R. F., & Szymkowiak, A. E. 1988, in *Cooling Flows in Clusters and Galaxies*, ed. A. C. Fabian (Dordrecht: Kluwer), 53  
 Pallavicini, R., Tagliaferri, G., & Stella, L. 1990, *A&A*, 228, 403  
 Pandel, D., & Córdova, F. A. 2002, *MNRAS*, 336, 1049  
 Pandel, D., Córdova, F. A., Shirey, R. E., Ramsay, G., Cropper, M., Mason, K. O., Much, R., & Kilkenny, D. 2002, *MNRAS*, 332, 116  
 Patterson, J., Lamb, D. Q., Fabbiano, G., Raymond, J. C., Beuermann, K., Swank, J., & White, N. E. 1984, *ApJ*, 279, 785  
 Ramsay, G., Cropper, M., & Mason, K. O. 1996, *MNRAS*, 278, 285  
 Reimers, D., & Hagen, H.-J. 2000, *A&A*, 358, L45  
 Reimers, D., Hagen, H.-J., & Hopp, U. 1999, *A&A*, 343, 157  
 Ritter, H. 1988, *A&A*, 202, 93  
 Rousseau, T., Fischer, A., Beuermann, K., & Woelk, U. 1996, *A&A*, 310, 526  
 Schneider, D. P., & Young, P. 1980, *ApJ*, 240, 871  
 Schwarz, R., Schwöpe, A. D., & Staudte, A. 2001, *A&A*, 374, 189  
 Schwöpe, A. D., & Beuermann, K. 1997, *Astron. Nachr.*, 318, 111  
 Shakhovskoy, N. M., Alexeev, I. Y., Andronov, I. L., & Kolesnikov, S. V. 1993, *Ann. Israel Phys. Soc.*, 10, 237  
 Sion, E. M. 1999, *PASP*, 111, 532  
 Sirk, M. M., & Howell, S. B. 1998, *ApJ*, 506, 824  
 Strüder, L., et al. 2001, *A&A*, 365, L18  
 Szkody, P., et al. 2003, *ApJ*, 583, 902  
 Tapia, S. 1977, *IAU Circ.*, 3054, 1  
 Thomas, H.-C., Beuermann, K., Schwöpe, A. D., & Burwitz, V. 1996, *A&A*, 313, 833  
 Turner, M. J. L., et al. 2001, *A&A*, 365, L27  
 Vennes, S., Szkody, P., Sion, E. M., & Long, K. S. 1995, *ApJ*, 445, 921  
 Walker, M. F. 1965, *Commun. Konkoly Obs.*, 57, 1  
 Warner, B. 1995, *Cataclysmic Variable Stars* (Cambridge: Cambridge Univ. Press)  
 Warren, J. K., Vallerger, J. V., Mauche, C. W., Mukai, K., & Siegmund, O. H. W. 1993, *ApJ*, 414, L69  
 Webb, N. A., Naylor, T., & Jeffries, R. D. 2002, *ApJ*, 568, L45  
 Woelk, U., & Beuermann, K. 1996, *A&A*, 306, 232